

G Protein–Coupled Estrogen Receptor Is Apoptotic and Correlates with Increased Distant Disease-Free Survival of Estrogen Receptor–Positive Breast Cancer Patients

Stefan Broselid¹, Benxu Cheng⁵, Martin Sjöström², Kristina Lövgren², Heather L.P. Klug-De Santiago⁵, Mattias Belting^{2,4}, Karin Jirström^{3,4}, Per Malmström^{2,4}, Björn Olde¹, Pär-Ola Bendahl², Linda Hartman², Märten Fernö², and L.M. Fredrik Leeb-Lundberg^{1,5}

Abstract

Purpose: G protein–coupled estrogen receptor 1 (GPER1), previously named GPR30, is a membrane receptor reported to mediate nongenomic estrogen responses. We investigated if GPER1 expression correlates with any clinicopathologic variables and distant disease-free survival (DDFS) in patients with breast cancer, if any prognostic impact of the receptor is dependent on estrogen receptor- α (ER- α) status, and if the receptor impacts apoptotic signaling in ER-positive breast cancer cells.

Experimental Design: GPER1 expression was analyzed by immunohistochemistry in breast tumors from 273 pre- and postmenopausal stage II patients, all treated with adjuvant tamoxifen for 2 years (cohort I) and from 208 premenopausal lymph node-negative patients, of which 87% were not subjected to any adjuvant systemic treatment (cohort II). GPER1-dependent proapoptotic signaling was analyzed in MCF7 cells with and without GPER1 knockdown, T47D cells, HEK293 cells (HEK), and HEK stably expressing GPER1 (HEK-R).

Results: GPER1 positively correlates with ER and progesterone receptor expression. Multivariate analysis showed that GPER1 is an independent prognostic marker of increased 10-year DDFS in the ER-positive subgroup. HEK-R has higher basal proapoptotic signaling compared with HEK including increased cytochrome C release, caspase-3 cleavage, PARP cleavage, and decreased cell viability. Treating HEK-R with the proteasome inhibitor epoxomicin, to decrease GPER1 degradation, further increases receptor-dependent proapoptotic signaling. Also, GPER1 knockdown decreases basal and agonist-stimulated proapoptotic receptor signaling in MCF7 cells.

Conclusions: GPER1 is a prognostic indicator for increased DDFS in ER-positive breast cancer, which may be associated with constitutive GPER1-dependent proapoptotic signaling in ER-positive breast cancer cells. *Clin Cancer Res*; 19(7); 1681–92. ©2013 AACR.

Introduction

Breast cancer is the most common female cancer constituting about 30% of all cancers in women (1). This cancer is

a heterogeneous disease with several subtypes with different biologic characteristics and clinical behaviors, which are traditionally divided on the basis of the presence of 3 receptors, estrogen receptor- α (ER- α), progesterone receptor (PgR), and HER2 (2). The presence of ER and HER2 allows targeted therapeutic intervention by blocking proliferative ER and HER2 signaling. Endocrine therapy with antiestrogens, for example, tamoxifen, has long been a therapeutic choice for all stages of ER-positive breast cancer. Tamoxifen acts by interfering with proliferative genomic estrogen signaling at ER, which functions as a nuclear transcription factor to regulate gene expression (3). However, a significant number of ER-positive breast cancers fail to respond to tamoxifen treatment (4) emphasizing the necessity for other therapeutic targets in this cancer.

G protein–coupled estrogen receptor 1 (GPER1), formerly known as GPR30 as an orphan, is a G protein–coupled receptor (GPCR) structurally distinct from ER that was reported to bind 17 β -estradiol (E2) with relatively high affinity and to mediate nongenomic responses to estrogen

Authors' Affiliations: ¹Department of Experimental Medical Science, ²Department of Clinical Science, Division of Oncology, and ³Department of Clinical Science, Division of Pathology, Lund University; ⁴Skåne Department of Oncology, Skåne University Hospital, Lund, Sweden; and ⁵Medical Research Division, Regional Academic Health Center, The University of Texas Health Science Center at San Antonio, Edinburg, Texas

Note: Supplementary data for this article are available at Clinical Cancer Research Online (<http://clincancerres.aacrjournals.org/>).

S. Broselid, B. Cheng, and M. Sjöström contributed equally as first authors. M. Fernö and L.M.F. Leeb-Lundberg contributed equally as last authors.

Corresponding Author: L.M. Fredrik Leeb-Lundberg, Department of Experimental Medical Science, Lund University, BMC, A12, SE-22184 Lund, Sweden. Phone: 46-46-2223944; Fax: 46-46-2220568; E-mail: fredrik.leeb-lundberg@med.lu.se

doi: 10.1158/1078-0432.CCR-12-2376

©2013 American Association for Cancer Research.

Translational Relevance

G protein-coupled estrogen receptor 1 (GPER1) is a novel putative membrane estrogen receptor (ER). Here, we investigated whether GPER1 correlates with any clinicopathologic variables and distant disease-free survival (DDFS) in patients with breast cancer. Two cohorts of patients with breast cancer were studied, one with stage II carcinoma subsequently treated with tamoxifen and another with lymph node-negative carcinoma subsequently mainly not treated with tamoxifen. GPER1 positively correlated with ER- α and progesterone receptor expression and with increased DDFS in ER-positive cancer. GPER1 was constitutively proapoptotic in ER-positive breast cancer cells. Therefore, GPER1 may be a novel prognostic marker in breast cancer, and enhancing GPER1-dependent proapoptotic signaling may be a therapeutic avenue in this disease.

in vivo (5–7) and *in vitro* (8, 9) and to tamoxifen *in vitro* (10, 11). However, the designation of E2 as the cognate GPER1 ligand is debated (12, 13). Nevertheless, GPER1 correlates with ER and PgR expression in breast tumors (14–17) and coimmunoprecipitates with ER in ER- and PgR-positive MCF7 cells (18), suggesting that GPER1 and ER are functionally related. GPER1 knockdown enhances E2-stimulated cell proliferation in MCF7 cells (17), and progesterone-promoted GPER1 upregulation is required for the antiproliferative progesterone response in these cells (19, 20). Because this occurs apparently independently of E2 (19, 20), GPER1 may be constitutively antiproliferative in ER-positive breast cancer cells. Indeed, GPER1 is constitutively apoptotic in rat cardiac cells (21), and E2-regulated GPER1 activity is either proapoptotic (22, 23) or antiapoptotic (24, 25) depending on the system studied.

Here, we investigated if GPER1 correlates with any clinicopathologic variables and distant disease-free survival (DDFS) in patients with breast cancer, if any prognostic impact of the receptor is dependent on ER status, and if the receptor impacts apoptotic signaling. Our results show that GPER1 correlates positively with ER and PgR expression, but not with HER2 expression, associates with increased DDFS in ER-positive breast cancer and is constitutively apoptotic in ER-positive breast cancer cells. Thus, GPER1 may be an interesting new prognostic marker and therapeutic target in ER-positive breast cancer.

Materials and Methods

Patients

Cohort I consisted of 273 patients, including 56 (21%) premenopausal and 217 (79%) postmenopausal (median age 62 years; range, 26–81), with stage II (pT2pN0pM0, pT1-2pN1pM0) breast carcinoma diagnosed in the South Sweden Health Care Region (1985–1994). The patients had previously been selected from 2 randomized clinical trials (26, 27) to compare methods for evaluation of hormone

receptor status (28). All patients were operated with modified radical mastectomy or breast-conserving surgery with axillary lymph node dissection (level I and II). After breast-conserving surgery, radiotherapy (50 Gy) was given to the breast. In patients with axillary lymph node metastases, locoregional radiotherapy was also administered. All patients were treated with tamoxifen for 2 years, irrespective of ER status. The median follow-up was 6.1 years for the endpoint DDFS for patients alive and free from distant metastases at the last review of the patients' records. No patients received any systemic adjuvant therapy besides tamoxifen.

Cohort II consisted of 237 premenopausal women with node-negative breast carcinoma diagnosed in the South Sweden Health Care Region (1991–1994). In 14 cases, no paraffin blocks were retrieved, 6 cases were excluded because of problems in preparation or staining, and 9 cases were excluded as the material only contained normal breast tissue or carcinoma *in situ*. Of the analyzed 208 patients (median age 47; range, 30–57), all patients received breast surgery and in most cases postoperative radiotherapy. Of these, 180 patients received no adjuvant systemic therapy after surgery, 7 patients received tamoxifen (20 mg daily for 5 years), 1 patient was oophorectomized, and 20 patients received chemotherapy (cyclophosphamide, methotrexate, and 5-fluorouracil i.v. 9 cycles). The median follow-up was 10.8 years for the endpoint DDFS for patients alive and free from distant metastases at the last review of the patients' records. Information on clinical outcome and patient- and tumor-related factors were reported previously (29).

Preparation of tissue microarrays

Tissue microarrays (TMA) were prepared from paraffin-embedded blocks using a manual arrayer (Beecher Instruments). Two 0.6-mm cores were taken from representative areas of each primary tumor block and transferred into a recipient paraffin block, constituting the TMA block. Sections (4 μ m) were cut from each TMA block and placed on glass slides (Menzel Superfrost Plus) and dried at 60°C for 2 hours.

Immunohistochemical staining

Deparaffinization and pretreatment was conducted in PT-Link (Dako) with Target Retrieval Solution pH 6. After blocking with peroxidase block S2023 (Dako) for 5 minutes, the slides were incubated with GPER1 antibody (R&D System, 1:50) for 60 minutes and then with K0690 (Dako) with a biotinylated secondary antibody followed by streptavidin-horseradish peroxidase (HRP). Peroxidase/DAB was used for visualization. Nuclear staining with Mayer's hematoxylin was done for contrast. These steps were carried out in an Autostainer plus staining machine (Dako). The slides were then washed in tap water for 10 minutes and dehydrated with ethanol and xylene. Glass coverslips were mounted with Pertex mounting medium.

Evaluation of immunohistochemical staining

Immunohistochemical staining was examined by light microscopy without knowledge of clinical and tumor

characteristic data. GPER1 antibody staining was estimated semi-quantitatively as the fraction of stained tumor cells (0%–1%, 2%–10%, 11%–50%, and 51%–100%) and the intensity of stained tumor cells was scored (0, no; 1, very weak; 2, weak; 3, moderate; and 4, strong). Two individuals examined all stained samples and final consensus was reached in any discrepant cases. In cohort I, 24 (8.8%) showed 0%–1% stained cells, 1 (0.4%) 2%–10%, 5 (1.8%) 11%–50%, and 243 (89%) more than 50%. In terms of staining intensity, 24 (8.8%) were judged negative (level 0), 38 (13%) very weak (level 1), 125 (46%) weak (level 2), 75 (28%) moderate (level 3), and 11 (4%) strong (level 4). In cohort II, 20 (9.6%) showed 0%–1% stained cells, 2 (1%) 2%–10%, 0 (0%) 11%–50%, and 186 (89%) more than 50%. In terms of staining intensity, 20 (10%) were level 0, 69 (33%) level 1, 87 (42%) level 2, 23 (11%) level 3, and 9 (4%) level 4.

Cell culture and DNA constructs

HeLa cells [American Type Culture Collection (ATCC)] and cells stably expressing GPER1 were made and grown as previously described (30). HEK293 cells (ATCC; HEK) and HEK stably expressing GPER1 tagged in the N terminus with the FLAG epitope (HEK-R) were made and grown as previously described (31). HEK were transiently transfected with cDNA for GPER1 tagged in the N terminus with the FLAG epitope (FGPER1) using TransIT-293 (Mirus). MCF7 cells (ATCC) were grown in Dulbecco's modified essential medium supplemented with 10% FBS in 5% CO₂ at 37°C. Two days before experimentation, cells were grown in 5% charcoal-treated FBS. MCF7 cells were infected with GPER1 short hairpin RNA (shRNA) lentiviral particles and stable clones were enriched using puromycin as described by the supplier (Santa Cruz).

Immunoblotting

Immunoblotting was done as previously described (32). Membranes were probed with antibodies from R&D Systems (GPER1), Sigma-Aldrich (M2 FLAG, β -actin), Biovision (cytochrome C), Cell Signaling (cleaved caspase-3, PARP, and ubiquitin), and Santa Cruz [p-ERK1/2, extracellular signal-regulated kinase (ERK)1/2, and p53]. Immunoreactive bands were visualized with a chemiluminescence immunodetection kit as described by the supplier (GE Healthcare).

Flow cytometry analysis

For cell surface receptor analysis, cells were collected and washed twice with ice-cold buffer (PBS with Ca²⁺/Mg²⁺–containing 10% FBS). Cells were resuspended in cold buffer, counted, and aliquoted at 5×10^5 cells/mL. The cells were then incubated with mouse M1 FLAG antibody (Sigma-Aldrich) at 4°C for 20 minutes, followed by further incubation with goat anti-mouse allophycocyanin (APC)-conjugated antibody (Life Technologies) at 4°C for 30 minutes in the dark. The cells were then fixed in PBS containing 2% formaldehyde before analysis by flow cytometry. The geometric mean fluorescence in the APC channel

for stained cells was measured by fluorescence-activated cell sorting (FACS) analysis on an LSRFortessa (BD Biosciences) using FACSDiva software version 6.1.2 (BD Biosciences) for data collection. FlowJo software version 7.6.4 (Tree Star) was used for analysis. For each sample, 3×10^4 events were collected and forward scatter (FSC) and side scatter (SSC) gates were set on the cell population. For all samples, greater than 85% of the events fell within the FSC/SSC gate. Statistical analysis was done using Excel software (Microsoft Office 2007).

For cell-cycle analysis, collected cells were briefly fixed for 30 minutes with 4% formaldehyde on ice. Cells were permeabilized by adding 5 mL of cold 70% ethanol dropwise while vortexing. Samples were stored at –20°C until staining with propidium iodide (PI)/RNase staining buffer (BD Biosciences) for 15 minutes at room temperature. Cell-cycle profiles were collected on 3×10^4 events per sample using the LSRFortessa (BD Biosciences). For data collection, FACSDiva software ver. 6.1.2 (BD Biosciences) was used. Statistical analysis was done using Excel software (Microsoft Office 2007).

Immunofluorescence microscopy

Fixed HEK transiently transfected with FGPER1 cDNA were stained and visualized using M1 FLAG antibody (Sigma-Aldrich) as primary antibody and Alexa488-labeled mouse immunoglobulin G (IgG)2b (Invitrogen) as secondary antibody, and images were collected using a Nikon Eclipse confocal fluorescence microscope as previously described (31). An antibody against endogenously expressed cytokeratin 8 (Sigma-Aldrich) and a secondary Alexa568-labeled mouse IgG1 antibody (Invitrogen) were used to distinguish transfected from untransfected cells.

Cell viability

Morphologic changes and nuclear staining of cells with Hoechst 33342 were determined by phase-contrast and fluorescence microscopy using a Leica 6000 B microscope. Cell viability was monitored by the conversion of MTT to formazan.

Statistical analysis

DDFS was visualized using the Kaplan–Meier method and the influence of GPER1 intensity (on 5 levels) on DDFS was tested using a log-rank test for trend. The Cox proportional hazards model was used for estimation of univariate and multivariate HRs and to investigate interactions between GPER1 and ER. GPER1 intensity on 5 levels (coded as 0–4) and age were used as linear covariates (i.e., test for trend), whereas all other factors were used as dichotomized covariates in the statistical analyses, except for histologic grade (3 groups). The HR for GPER1 as a linear covariate is then a mean change for 1 step on the linear GPER1 intensity scale. Proportional hazards assumptions were checked both graphically and using Schoenfeld test (33). To check the assumptions of linear trend for GPER1, we compared the linear Cox-model with a Cox-model with GPER1 as a factor on 5 levels. For the established prognostic factors, standard

cutoff values were used and were the same as for earlier published patient series (29, 34). Association between GPER1 and the other factors were analyzed using Pearson χ^2 test for trend. All *P* values correspond to 2-sided tests. The statistical calculations were conducted using Stata version 11.0 (StataCorp 2009).

Ethical considerations

This project was approved by the ethical committee at Lund University (Lund, Sweden; LU 240-01). All information and data were handled confidentially. Full consent was obtained from patients involved in the study for patient participation and for publication of study results.

Results

GPER1 expression correlates with ER-positive breast tumors

GPER1 was evaluated by immunohistochemical staining of breast tumors from 2 patient cohorts using a GPER1-specific antibody. The specificity of the receptor antibody was validated in HeLa cells, with naïve cells (HeLa), which do not express GPER1, lacking immunoreactivity, and HeLa cells stably expressing the receptor (HeLa-GPER1) showing an immunoreactive band of a molecular mass (40 kDa) corresponding to the predicted mass of the receptor (Fig. 1A).

Because approximately 90% of the tumor samples had more than 50% stained cells, staining intensity at 5 levels (Fig. 1B, a–e) rather than staining fraction was used for further analysis. In cohort I, consisting of 273 pre- and postmenopausal stage II cases subsequently treated with tamoxifen, tumors with higher GPER1 were more likely to be ER-positive ($P = 0.01$) and PgR-positive ($P = 0.01$) but did not correlate with any other clinicopathologic variable including age, lymph node status, tumor size, histologic grade, HER2 expression, and Ki67 staining (Table 1). In cohort II, consisting of 208 premenopausal node-negative breast cancer cases subsequently mainly not subjected to adjuvant systemic treatment, tumors with higher GPER1 intensity were also more likely to be positive for ER ($P = 0.0005$) and PgR ($P = 0.0004$) and again did not correlate with HER2 (Table 1). However, GPER1 correlated positively with increasing age ($P = 0.003$) and negatively with large tumor size ($P = 0.05$), high histologic grade ($P = 0.0003$), and high Ki67 staining ($P = 0.0007$; Table 1).

GPER1 expression correlates with increased DDFS in patients with ER-positive breast tumors

With 10 years of follow-up for survival and distant metastases, 81 patients were diagnosed with distant recurrences in cohort I. In this cohort, GPER1 significantly correlated with increased DDFS ($P = 0.014$; log-rank test for trend; Fig. 1C). A Cox-model for univariate analysis with GPER1 as a linear covariate gave HR = 0.75 [95% confidence interval (CI), 0.60–0.94], which should be interpreted as the mean HR for an arbitrary step on the scale (0–4). Testing this model against the more flexible model treating GPER1 as a

factor on 5 levels, did not contradict this interpretation ($P = 0.3$). Schoenfeld test did not indicate departure from the assumption of proportional hazards. When stratifying for ER status, GPER1 was a significant prognostic factor in the ER-positive subgroup (HR, 0.66; 95% CI, 0.49–0.88; $P = 0.007$; Fig. 1C; Table 2) but not in the ER-negative subgroup (HR, 1.06; 95% CI, 0.76–1.48; $P = 0.7$; Fig. 1C). In a Cox-model allowing for interaction between GPER1 as a linear covariate and ER-status, we achieved moderate evidence of interaction ($P = 0.06$). Consistent with the whole cohort, GPER1 did not correlate with any other clinicopathologic variable in the ER-positive subgroup (Supplementary Table S1). Further multivariate analysis revealed that GPER1 was a significant independent prognostic factor in the ER-positive subgroup (HR, 0.67; 95% CI, 0.50–0.92; $P = 0.01$; Table 2). The HR for GPER1 remained relatively constant and significant in the multivariate analysis regardless of which additional variables indicated in Table 2 that were included in the model (data not shown).

In cohort II, 46 patients were diagnosed with distant recurrences within 10 years. Analysis of this cohort revealed a trend toward increased 10-year DDFS in patients with higher GPER1-expressing tumors ($P = 0.08$; log-rank test for trend; Fig. 1D). A Cox-model for univariate analysis with GPER1 as a linear covariate gave HR = 0.75 (95% CI, 0.55–1.04), and treating GPER1 as a factor on 5 levels did not significantly improve the fit ($P = 0.8$). With GPER1 as a linear covariate, Schoenfeld test gave modest evidence ($P = 0.06$) for departure from the assumption of proportional hazards, in which case the HR should be interpreted as a mean HR over the time-period studied rather than constant at all times. When stratifying for ER status, the trend was again observed in the ER-positive subgroup (HR, 0.62; 95% CI, 0.39–0.99; $P = 0.047$; Fig. 1D; Table 3) but not in the ER-negative subgroup (HR, 0.97; 95% CI, 0.63–1.49; $P = 0.89$; Fig. 1D) but the interaction was not statistically significant ($P = 0.16$). In the ER-positive subgroup, GPER1 remained negatively associated with high histologic grade ($P = 0.02$) and high Ki67 staining ($P = 0.05$) but not with any other clinicopathologic variables (Supplementary Table S1). The prognostic value of GPER1 did not remain significant in multivariate analysis of this subgroup (HR, 0.60; 95% CI, 0.34–1.1; $P = 0.09$; Table 3). Indeed, due to the large number of factors included, and the colinearity between them, no established risk factor was significant in this multivariate model. However, the HR for GPER1 in this subgroup was comparable with that in cohort I and again remained relatively constant regardless of which additional variables indicated in Table 3 that were included in the model (data not shown). This suggests that GPER1 has added prognostic value, and that the lack of significance is due in part to the smaller number of cases and recurrences available for analysis in this subgroup (34 in cohort I and 18 in cohort II). Similar results were obtained when only the 180 systemically untreated patients were analyzed in cohort II (data not shown). However, due to fewer events, the *P* values were higher for this subgroup than for the entire cohort.

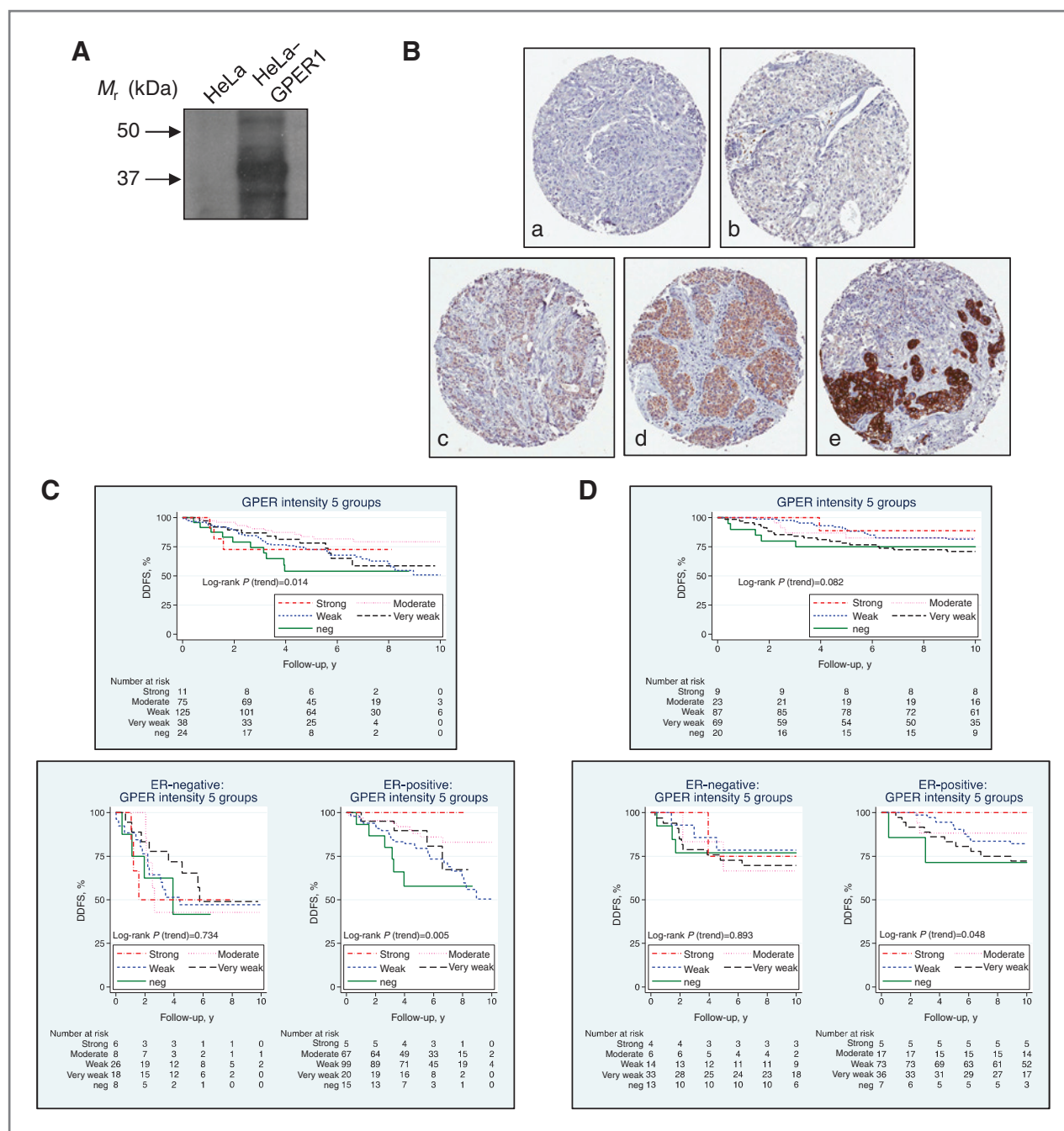


Figure 1. GPER1 expression correlates with increased DDFS in ER-positive breast cancer. **A**, GPER1 antibody specificity as determined by immunoblotting HeLa cells without (*HeLa*) and with stable expression of human GPER1 (*HeLa-GPER1*). Molecular mass (M_r) standards (kDa; left side arrows) are indicated. **B**, levels of GPER1 immunostaining intensity in invasive breast cancer in cohort II. Representative images show intensity levels as negative (level 0; a), very weak (level 1; b), weak (level 2; c), moderate (level 3; d), and strong (level 4; e). **C**, Kaplan-Meier estimates of DDFS for GPER1 status in the whole cohort I and the ER-positive and -negative subgroups of cohort I. **D**, Kaplan-Meier estimates of DDFS for GPER1 status in the whole cohort II and the ER-positive and ER-negative subgroups of cohort II. P values were calculated using the log-rank test for trend. Below each graph is the number of patients remaining at risk in each group at each time.

GPER1 is constitutively proapoptotic in a HEK293 cell model system

Because GPER1 was found to be of clinical benefit both with and without tamoxifen treatment, we first investigated

if the receptor constitutively impacts proapoptotic signaling, that is, without added stimulus. To do this requires comparing cells completely lacking GPER1 expression with the same cells stably expressing the receptor. To this end, we

Downloaded from <http://aacrjournals.org/clinccancerres/article-pdf/19/7/1681/2299205/1681.pdf> by guest on 01 December 2024

Table 1. Association between GPER1 intensity score and various clinicopathologic variables in cohorts I and II

Factor	Cohort I						<i>P</i> ^a	Cohort II						<i>P</i> ^a
	GPER1 intensity							GPER1 intensity						
	Patient 0	1	2	3	4	<i>N</i>		Patient 0	1	2	3	4	<i>N</i> (%)	
All	273	24 (9)	38 (14)	125 (46)	75 (27)	11 (4)		208	20 (10)	69 (33)	87 (42)	23 (11)	9 (4)	
Age, years							0.18							0.003
Node status														
Negative	89	8 (9)	16 (18)	30 (34)	26 (29)	9 (10)	0.26							
Positive	183	16 (9)	22 (12)	94 (51)	49 (27)	2 (1)								
Missing	1													
Tumor size														
≤20 mm	80	5 (6)	12 (15)	42 (53)	21 (26)	0 (0)	0.56	155	10 (6)	51 (33)	69 (45)	18 (12)	7 (5)	0.05
>20 mm	193	19 (10)	26 (13)	83 (43)	54 (28)	11 (6)		53	10 (19)	18 (34)	18 (34)	5 (9)	2 (4)	
Histologic grade														
1	15	0 (0)	1 (7)	6 (40)	8 (53)	0 (0)	0.88	62	0 (0)	16 (26)	34 (55)	10 (16)	2 (3)	0.0003
2	176	19 (11)	18 (10)	89 (51)	45 (26)	5 (3)		77	5 (6)	25 (32)	39 (51)	6 (8)	2 (3)	
3	73	3 (4)	17 (23)	27 (37)	20 (27)	6 (8)		67	15 (22)	28 (42)	13 (19)	6 (9)	5 (7)	
Missing	9							2						
ER														
Positive	206	15 (7)	20 (10)	99 (48)	67 (33)	5 (2)	0.01	138	7 (5)	36 (26)	73 (53)	17 (12)	5 (4)	0.0005
Negative	66	8 (12)	18 (27)	26 (39)	8 (12)	6 (9)		70	13 (19)	33 (47)	14 (20)	6 (9)	4 (6)	
Missing	1													
PgR														
Positive	164	11 (7)	16 (10)	76 (46)	57 (35)	4 (2)	0.01	151	10 (7)	39 (26)	79 (52)	19 (13)	4 (3)	0.0004
Negative	108	12 (11)	22 (20)	49 (45)	18 (17)	7 (6)		57	10 (18)	30 (53)	8 (14)	4 (7)	5 (9)	
Missing	1													
HER2														
Negative	206	16 (8)	30 (15)	92 (45)	57 (28)	11 (5)	0.76	173	17 (10)	52 (30)	77 (45)	19 (11)	8 (5)	0.45
Positive	34	2 (6)	4 (12)	19 (56)	9 (26)	0 (0)		22	1 (5)	11 (50)	7 (32)	3 (14)	0 (0)	
Missing	43							13						
Ki67														
Low (≤20%)	170	13 (8)	20 (12)	80 (47)	51 (30)	6 (4)	0.24	127	7 (6)	31 (24)	69 (54)	16 (13)	4 (3)	0.0007
High (>20%)	97	9 (9)	17 (18)	44 (45)	23 (24)	4 (4)		60	9 (15)	32 (53)	11 (18)	5 (8)	3 (5)	
Missing	6							21						

^aTest for zero slope in a linear regression, which equals a χ^2 test for trend for binary variables.

compared naïve HEK293 cells (HEK) with HEK stably expressing GPER1 (HEK-R; Fig. 2A), a well-studied GPCR model system. HEK-R had a $35\% \pm 2\%$ ($P < 0.001$) decrease in cell viability compared with HEK as determined by the MTT assay (Fig. 2A). Consistent with constitutive proapoptotic receptor signaling, HEK-R also had increased basal mitochondrial cytochrome C release, an early marker of apoptosis (Fig. 2B, EPX: 0 nmol/L). Caspase-3 cleavage was not detected under basal conditions in either HEK or HEK-R, but HEK-R had increased basal PARP cleavage, a product of caspase-3 activity, and increased ERK1/2 phosphorylation (p-ERK1/2; Fig. 2B, EPX: 0 nmol/L).

Epoxomicin (EPX) is a specific proteasomal inhibitor and apoptotic stimulant as shown by increased protein ubiquitination, cytochrome C release, and PARP cleavage in HEK

following treatment with 50 and 100 nmol/L epoxomicin for 24 hours (Fig. 2B, epoxomicin: 50,100 nmol/L). Epoxomicin is also expected to increase the level of GPER1 by blocking proteasomal receptor degradation (35). Indeed, epoxomicin treatment of HEK-R increased the level of GPER1 at the cell surface as shown by both flow cytometry (Fig. 2C) and confocal immunofluorescence microscopy (Supplementary Fig. S1). Consistent with constitutive proapoptotic GPER1 signaling, epoxomicin treatment of HEK-R also yielded levels of cytochrome C release, caspase-3 cleavage, and PARP cleavage that were significantly higher than in epoxomicin-treated HEK (Fig. 2B, epoxomicin: 50,100 nmol/L). The higher level of proapoptotic signaling in HEK-R was also evident by the increased morphologic changes and chromatin condensation/nuclear fragmentation in

Table 2. DDFS by Cox univariate and multivariate analysis in the ER-positive subgroup of cohort I

Variable	Univariate DDFS			Multivariate DDFS		
	N	HR (95% CI)	P	N	HR (95% CI)	P
Age (linear, y)	206	0.99 (0.97–1.02)	0.62	199	1.00 (0.97–1.03)	0.93
GPER1 (trend)	206	0.66 (0.49–0.88)	0.007	199	0.67 (0.50–0.92)	0.01
Node status (N+ vs. N0)	206	1.23 (0.66–2.28)	0.52	199	1.60 (0.83–3.07)	0.16
Tumor size (>20 mm vs. ≤20 mm)	206	1.95 (0.95–4.02)	0.05	199	2.22 (1.04–4.72)	0.04
Histologic grade	202		0.18 ^a	199		0.46 ^a
1 vs. 3		0.22 (0.03–1.76)	0.16		0.45 (0.05–3.80)	0.46
2 vs. 3		0.93 (0.45–1.93)	0.85		1.24 (0.55–2.81)	0.60
HER2 (pos vs. neg)	181	0.96 (0.38–2.46)	0.93	— ^b	—	—
PgR (pos vs. neg)	206	0.84 (0.45–1.59)	0.60	199	0.99 (0.51–1.94)	0.98
Ki67 (>20% vs. ≤20%)	203	2.02 (1.15–3.56)	0.02	199	2.01 (1.05–3.88)	0.04

^aP value for histologic grade as a factor on 3 levels.

^bHER2 excluded because of a higher frequency of missing data than the other variables.

these cells (Fig. 2D). Thus, GPER1 is constitutively proapoptotic and sensitizes cells to additional apoptotic stimulation in a model system.

GPER1 is proapoptotic in ER-positive breast cancer cells

Next, we evaluated if GPER1 is constitutively proapoptotic in ER-positive breast cancer cells. This was done by comparing naïve MCF7 cells with cells in which GPER1 had been knocked down with shRNA (MCF7-shRNA; Fig. 3A). Consistent with constitutive GPER1 signaling, receptor knockdown decreased basal p53 expression (Fig. 3B, G₁:0 μmol/L), a tumor suppressor protein associated with both increased apoptosis and decreased cell-cycle progression (36). No difference was observed in basal PARP cleavage and ERK1/2 phosphorylation (Fig. 3B). On the other hand, MCF7-shRNA had decreased cytochrome C release (Fig. 3B,

4OHT: 0 μmol/L). We conclude from these results that GPER1 is constitutively proapoptotic in MCF7 cells.

Proapoptotic GPER1 signaling in MCF7 cells was also investigated using G₁, a commercially available synthetic GPER1 agonist, keeping in mind that while this substance has been reported to be a receptor agonist (37), receptor-independent effects on, for example, cell-cycle progression has also been reported (38, 39). Stimulation with 1 μmol/L G₁ for 24 hours increased cytochrome C release, p53, PARP cleavage, and ERK1/2 phosphorylation (Fig. 3B) and decreased cell viability (Fig. 3C), the latter 4 responses clearly attenuated in MCF7-shRNA cells (Fig. 3B and C). We also determined the effect of G₁ in ER-positive T47D cells, which express significantly less GPER1 than MCF7 cells (40). Consistent with GPER1-dependent signaling, T47D cells were also much less sensitive than MCF7 cells to G₁-stimulated cytochrome C release and PARP cleavage

Table 3. DDFS by Cox univariate and multivariate analysis in the ER-positive subgroup of cohort II

Variable	Univariate DDFS			Multivariate DDFS		
	N	HR (95% CI)	P	N	HR (95% CI)	P ^b
Age (linear, y)	138	0.90 (0.84–0.96)	0.002	120	0.88 (0.82–0.95)	0.001
GPER1 (trend)	138	0.62 (0.39–0.99)	0.05	120	0.60 (0.34–1.1)	0.09
Tumor size (>20 mm vs. ≤20 mm)	138	1.1 (0.44–2.7)	0.85	120	0.78 (0.30–2.0)	0.60
Histologic grade	136		0.02 ^a	120		0.59 ^a
1 vs. 3		0.28 (0.11–0.73)	0.01		0.65 (0.17–2.6)	0.54
2 vs. 3		0.34 (0.14–0.82)	0.02		0.53 (0.16–1.8)	0.31
HER2 (pos vs. neg)	132	2.4 (0.85–7.1)	0.14	120	0.77 (0.23–2.5)	0.66
PgR (pos vs. neg)	138	0.88 (0.21–3.7)	0.87	120	4.5 (0.81–25.1)	0.09
Ki67 (>20% vs. ≤20%)	124	3.9 (1.8–8.6)	0.002	120	3.3 (1.0–10.6)	0.05

^aP value for histologic grade as a factor on 3 levels.

^bFor some factors, the much higher P values in multivariate analysis, compared with univariate analysis, can be explained by a high degree of colinearity between the variables in the model.

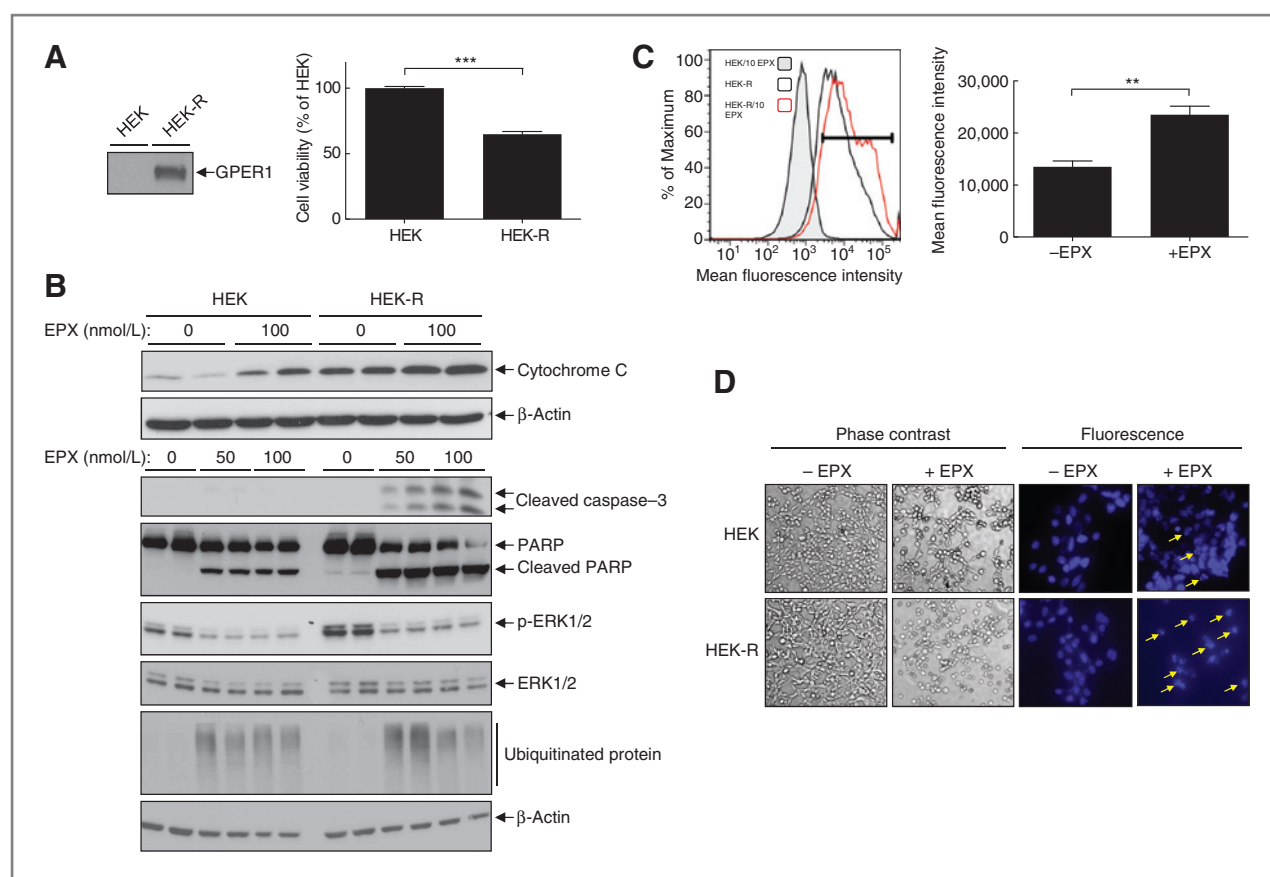


Figure 2. Constitutive proapoptotic GPER1 signaling in a HEK293 cell model system. **A**, immunoblotting of heterologously expressed GPER1 in HEK-R but not in HEK, and decreased cell viability of HEK-R compared with HEK as determined by the MTT assay (**B**), immunoblotting of cytochrome C release, cleaved caspase-3, cleaved PARP, phosphorylated ERK1/2 (p-ERK1/2), and ubiquitinated protein in HEK and HEK-R treated without and with different concentrations of epoxomicin for 24 hours as indicated. Duplicate samples were immunoblotted and total ERK1/2 and β -actin serve as loading controls. **C**, mean fluorescence intensity determined by flow cytometry of HEK and HEK-R labeled with primary mouse M1 FLAG antibody and secondary goat anti-mouse APC-labeled antibody. Before analysis, HEK were treated with 10 nmol/L epoxomicin (HEK/10 EPX), and HEK-R were treated without (HEK-R) and with 10 nmol/L epoxomicin for 24 hours (HEK-R/10 EPX). In this representative experiment, M1 FLAG-positive gate is shown (bar), and the percentage positive cells and mean fluorescence intensity was 1.1% and 5,679, respectively, for HEK/10 epoxomicin, 67.3% and 14,500, respectively, for HEK-R, and 78.4% and 24,500 for HEK-R/10 epoxomicin. Quantification of mean fluorescence intensity is also shown. **D**, morphologic changes as determined by phase-contrast and chromatin condensation/nuclear fragmentation as determined by Hoechst 33342 staining fluorescence following treatment of HEK and HEK-R without (-EPX) and with 50 nmol/L epoxomicin (+EPX) for 24 hours. Yellow arrows indicate fragmented nuclei. **, $P < 0.01$; ***, $P < 0.001$.

(Supplemental Fig. S2). Thus, agonist-stimulated GPER1 activity is proapoptotic in MCF7 cells.

G_1 treatment for 24 hours also inhibited MCF7 cell-cycle progression at the G_2 -M interphase in a GPER1-dependent manner (Fig. 3D and Supplemental Fig. S3), consistent with GPER1 mediating an increase in the p53 level and p53 blocking the cell cycle at this point (41). G_1 also changed cell morphology and increased the number of cells with fragmented nuclei (Fig. 3D).

We also investigated if GPER1 mediates any proapoptotic tamoxifen effects in MCF7 cells, noting again that this is complicated in an ER-positive environment because tamoxifen is also an ER antagonist, which in turn could impact apoptotic signaling. Nevertheless, 4-hydroxytamoxifen (4OHT), the active metabolite of tamoxifen, dose-dependently increased cytochrome C release and PARP cleavage in naïve MCF7 cells (Fig. 3B). These responses were lower in MCF7-

shRNA cells suggesting that they are at least in part GPER1-dependent. In analogy with G_1 and consistent with GPER1-dependence, the 4OHT effects were significantly lower in T47D cells (Supplemental Fig. S2). These results suggest that tamoxifen is proapoptotic in MCF7 cells in part via GPER1.

Discussion

Here, we show that GPER1 positively correlates with ER and PgR expression and with increased DDFS in ER-positive lymph node-negative and stage II breast cancer. GPER1 constitutively promotes proapoptotic signaling as determined in ER- and PgR-positive MCF7 cells and in a HEK model system stably expressing the receptor, which may explain in part the beneficial value of GPER1 on DDFS in ER-positive breast cancer.

More than 80% of breast cancers are positive for ER, emphasizing the importance of this receptor in cancer

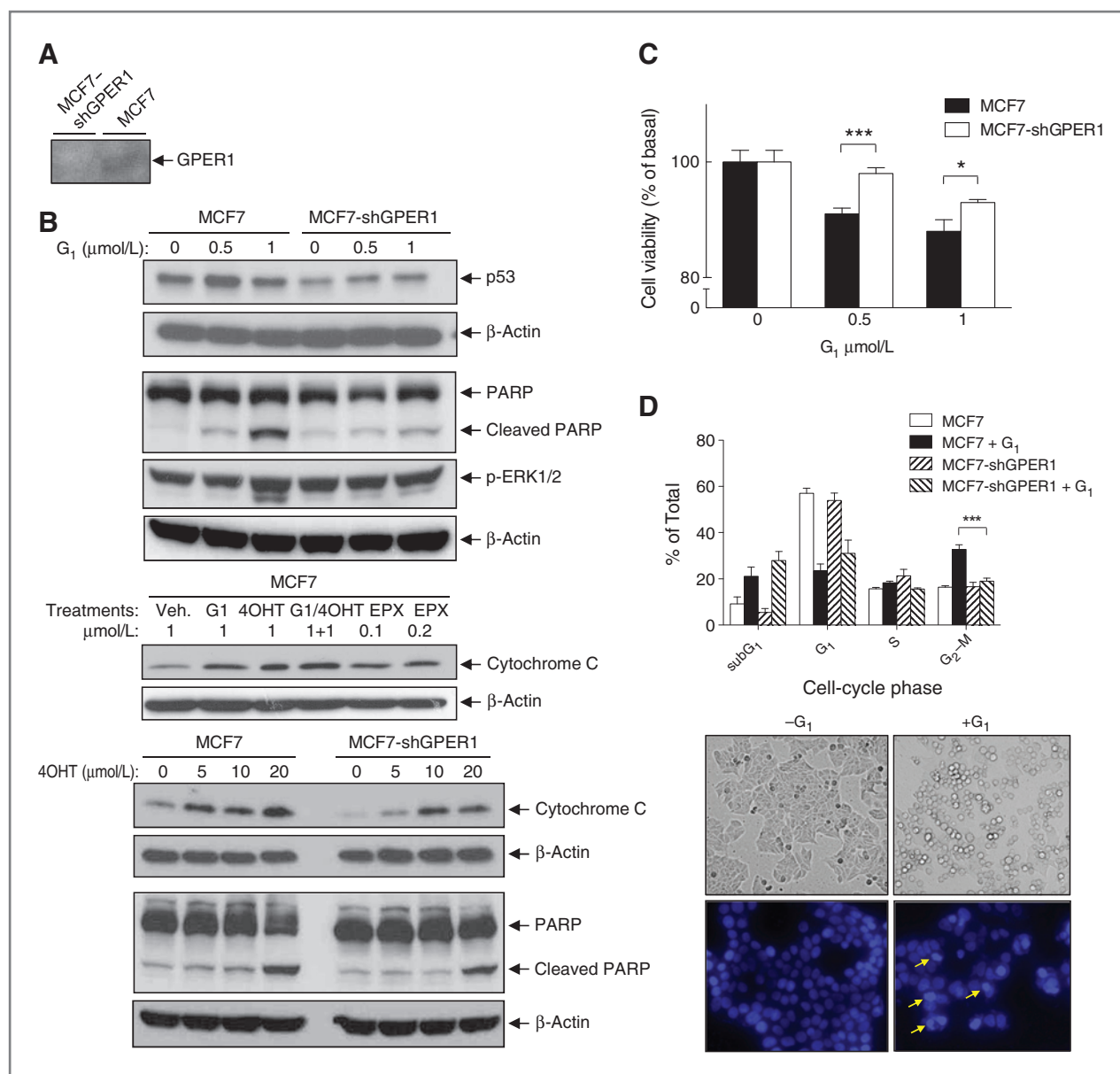


Figure 3. Constitutive and agonist-stimulated proapoptotic GPER1 signaling in MCF7 cells. **A**, immunoblotting of GPER1 in MCF7 cells without (*MCF7*) and with GPER1 shRNA knockdown (*MCF7-shGPER1*). **B**, immunoblotting of p53, cleaved PARP, phosphorylated ERK1/2 (p-ERK1/2), and cytochrome C release in MCF7 cells without (*MCF7*) and with GPER1 shRNA knockdown (*MCF7-shGPER1*) and treated with different concentrations of G_1 (G_1), 4OHT, and EPX for 24 hours as indicated. β -Actin serves as a loading control. **C**, viability of MCF7 cells without (*MCF7*) and with GPER1 shRNA knockdown (*MCF7-shGPER1*) and treated without and with increasing concentrations of G_1 for 24 hours as determined with the MTT assay. **D**, cell-cycle phases in MCF7 cells without (*MCF7*) and with GPER1 shRNA knockdown (*MCF7-shGPER1*) and treated without and with 1 $\mu\text{mol/L}$ G_1 for 24 hours as determined by flow cytometry, and morphologic changes and chromatin condensation/nuclear fragmentation as determined by Hoechst 33342 staining in MCF7 cells following treatment without ($-G_1$) and with 1 $\mu\text{mol/L}$ G_1 ($+G_1$) for 24 hours. Yellow arrows indicate fragmented nuclei. *, $P < 0.05$; ***, $P < 0.001$.

progression. We found a positive correlation of GPER1 with ER and PgR in 2 Swedish breast cancer cohorts, a stage II cohort (cohort I) and a lymph node-negative cohort (cohort II), which is consistent with data obtained on other cohorts by Filardo and colleagues (14) and Liu and colleagues (15) analyzing receptor protein by immunohistochemistry and by Kuo and colleagues (16) and Ariazi and colleagues (17) analyzing receptor transcript. In neither cohort analyzed in

our study did GPER1 correlate with HER2 expression. However, in cohort II GPER1 expression correlated negatively with several clinicopathologic markers for advanced disease and metastasis, whereas in cohort I it did not correlate with any of these markers. The reason for this cohort difference is not known but may be related to the menopausal stage because most (79%) patients in cohort I were postmenopausal, whereas all patients in cohort II were

Downloaded from <http://aacrjournals.org/clinccancerres/article-pdf/19/7/1681/2299205/1681.pdf> by guest on 01 December 2024

premenopausal. Another difference is that patients in cohort I were diagnosed before the introduction of mammographic screening, mostly with tumors greater than 20 mm, whereas patients in cohort II were diagnosed during the screening period, mostly with tumors smaller than 20 mm. Kuo and colleagues (16) and Tu and colleagues (42) also found no correlation with HER2 and with markers of poor prognosis. On the other hand, Filardo and colleagues (14), Liu and colleagues (15), and Ignatov and colleagues (43) found a positive correlation with HER2 as well as with various indicators of poor prognosis. The reason for this difference is also unknown but may be related to the composition of the various cohorts with patients of different ethnical and lifestyle backgrounds. Nevertheless, an association between GPER1 expression and ER-positive breast cancer is a consistent observation in clinical studies.

Reports that GPER1 associates with indicators of poor prognosis have led some investigators to propose that this receptor is linked to cancer progression (14, 43). However, the *GPER1* gene has not appeared in any gene expression profiles for aggressive breast cancer (44). Indeed, in our study with 2 cohorts, GPER1 correlated with increased DDFS. This correlation was specifically associated with the ER-positive groups. Furthermore, multivariate analysis showed that GPER1 has independent prognostic value in this subgroup. Consistent with our results, Ignatov and colleagues (43) also found that GPER1 significantly correlated with increased relapse-free survival in patients with breast cancer on no adjuvant treatment. Furthermore, Krakstad and colleagues (45) found the loss of GPER1 in a subgroup of ER-positive endometrial cancer to be associated with decreased survival. These results argue that GPER1 expression is a marker for good prognosis in ER-positive cancer.

Therapeutic activation of apoptosis in cancer cells is an attractive anticancer strategy. In HEK, a well-defined model system for studying GPCR function, GPER1 expression yielded increased proapoptotic signaling, whereas GPER1 knockdown in MCF7 cells yielded decreased signaling. These results show not only that GPER1 is proapoptotic in ER-positive breast cancer cells, but also that such receptor signaling occurs constitutively in the absence of any added stimulus, which may explain the beneficial clinical effect of GPER1 both in the absence and presence of adjuvant treatment. GPER1 expression also made HEK cells significantly more sensitive to apoptotic effects by the proteasomal inhibitor epoxomicin. This increased sensitivity was associated with an increased number of functional GPER1 in the plasma membrane rather than with accumulation of overexpressed receptors in the endoplasmic reticulum, a potential artificial cause of cellular stress and apoptosis. Thus, promoting cellular receptor expression and/or stabilizing GPER1 in the plasma membrane for example by decreasing constitutive receptor endocytosis and degradation may be a novel therapeutic avenue in ER-positive breast cancer. Hypoxia upregulates GPER1 expression, which in turn may increase constitutive apoptotic GPER1 signaling as previously described in cardiac cells (21). The GPER1 ago-

nist G_1 stimulated receptor-dependently proapoptotic signaling in MCF7 cells suggesting that direct receptor activation may be an alternative therapeutic approach in this disease.

Some investigators have suggested that GPER1 contributes to tamoxifen resistance based on observations that tamoxifen stimulates GPER1 *in vitro* (10, 11) and that GPER1 is upregulated in tamoxifen-resistant MCF7 cells (46). However, GPER1 has not appeared in functional screens for genes contributing to tamoxifen-resistance in breast cancer cells (47, 48). In our study, the prognostic value of GPER1 for increased DDFS was significant in both the tamoxifen-treated cohort I and the mainly untreated cohort II. Thus, no clear predictive value for the outcome of tamoxifen treatment can be assigned to GPER1 based on our study. Nevertheless, we found that tamoxifen stimulates proapoptotic signaling in MCF7 cells in part through GPER1, suggesting that it could potentially contribute to the beneficial clinical effects in our study. However, Ignatov and colleagues (43) found a negative correlation of GPER1 with relapse-free survival in patients treated with tamoxifen that was significantly different from their control group on no adjuvant treatment. Thus, assignment of GPER1 as a predictive factor for the outcome of tamoxifen treatment needs to be further investigated.

In summary, we show that GPER1 positively correlates with ER and PgR expression and with increased DDFS in ER-positive lymph node-negative and stage II breast cancer. Furthermore, GPER1 is proapoptotic in several cell types including ER-positive breast cancer cells. Therefore, expression of GPER1 may be a novel prognostic factor in this breast cancer, and enhancing GPER1 signaling in ER-positive breast tumors may present a novel therapeutic avenue to increase survival of patients with this disease.

Disclosure of Potential Conflicts of Interest

No potential conflicts of interest were disclosed.

Authors' Contributions

Conception and design: S. Broselid, B. Cheng, M. Sjöström, M. Belting, B. Olde, P.-O. Bendahl, M. Fernö, L.M.F. Leeb-Lundberg

Development of methodology: B. Cheng, M. Fernö

Acquisition of data (provided animals, acquired and managed patients, provided facilities, etc.): S. Broselid, M. Sjöström, H.L.P. Klug-De Santiago, K. Jirstrom, P. Malmström, M. Fernö

Analysis and interpretation of data (e.g., statistical analysis, biostatistics, computational analysis): S. Broselid, B. Cheng, M. Sjöström, H.L.P. Klug-De Santiago, P.-O. Bendahl, L. Hartman, M. Fernö, L.M.F. Leeb-Lundberg

Writing, review, and/or revision of the manuscript: S. Broselid, B. Cheng, M. Sjöström, H.L.P. Klug-De Santiago, M. Belting, K. Jirstrom, P. Malmström, B. Olde, P.-O. Bendahl, L. Hartman, M. Fernö, L.M.F. Leeb-Lundberg

Administrative, technical, or material support (i.e., reporting or organizing data, constructing databases): B. Cheng, K. Lövgren, M. Belting, M. Fernö

Study supervision: M. Fernö, L.M.F. Leeb-Lundberg

Acknowledgments

The authors thank the participating departments of the South Sweden Breast Cancer Group for providing us with breast cancer samples and clinical follow-up data. The expert technical assistance by J. Daszkiewicz-Nilsson is highly appreciated.

Grant Support

The study was supported by funds from the Swedish Research Council, Swedish Cancer Society, Gunnar, Arvid, and Elisabeth Nilsson Foundation, Mrs. Berta Kamprad Foundation, the University Hospital of Lund Research Foundation, the Anna and Edwin Bergers Foundation, Skåne County Council's Research and Development Foundation, Governmental Funding of Clinical Research within the National Health Service, and Regional Academic Health Center, The University of Texas Health Science Center at San Antonio.

The costs of publication of this article were defrayed in part by the payment of page charges. This article must therefore be hereby marked *advertisement* in accordance with 18 U.S.C. Section 1734 solely to indicate this fact.

Received July 18, 2012; revised December 21, 2012; accepted January 7, 2013; published online April 3, 2013.

References

- Kamangar F, Dores GM, Anderson WF. Patterns of cancer incidence, mortality, and prevalence across five continents: defining priorities to reduce cancer disparities in different geographic regions of the world. *J Clin Oncol* 2006;24:2137–50.
- Weigelt B, Peterse JL, van 't Veer LJ. Breast cancer metastasis: markers and models. *Nat Rev Cancer* 2005;5:591–602.
- Heldring N, Pike A, Andersson S, Matthews J, Cheng G, Hartman J, et al. Estrogen receptors: how do they signal and what are their targets. *Physiol Rev* 2007;87:905–31.
- Early Breast Cancer Trialists' Collaborative Group (EBCTCG) Davies C, Godwin J, Gray R, Clarke M, Cutter D, et al. Relevance of breast cancer hormone receptors and other factors to the efficacy of adjuvant tamoxifen: patient-level meta-analysis of randomised trials. *Lancet* 2011;378:771–84.
- Mårtensson UEA, Salehi SA, Windahl S, Gomez MF, Swärd K, Wendt A, et al. Deletion of the G protein-coupled receptor GPR30 impairs glucose tolerance, reduces bone growth, increases blood pressure, and eliminates estradiol-stimulated insulin release in female mice. *Endocrinology* 2009;150:687–98.
- Windahl SH, Andersson N, Chagin AS, Mårtensson UEA, Carlsten H, Olde B. The role of the G protein-coupled receptor GPR30 in the effects of estrogen in ovariectomized mice. *Am J Physiol* 2009;296:E490–6.
- Olde B, Leeb-Lundberg LMF. GPR30/GPER1: searching for a role in estrogen physiology. *Trends Endocrinol Metab* 2009;20:409–16.
- Thomas P, Pang Y, Filardo EJ, Dong J. Identity of an estrogen membrane receptor coupled to a G protein in human breast cancer cells. *Endocrinology* 2005;146:624–32.
- Revankar CM, Cimino DF, Sklar LA, Arterburn JB, Prossnitz ER. A transmembrane intracellular estrogen receptor mediates rapid cell signaling. *Science* 2005;307:1625–30.
- Maggiolini M, Vivacqua A, Fasanella G, Recchia AG, Sisci D, Pezzi V, et al. The G protein-coupled receptor GPR30 mediates c-fos up-regulation by 17beta-estradiol and phytoestrogens in breast cancer cells. *J Biol Chem* 2004;279:27008–16.
- Vivacqua A, Bonofiglio D, Recchia AG, Musti AM, Picard D, Andò S, et al. The G protein-coupled receptor GPR30 mediates the proliferative effects induced by 17beta-estradiol and hydroxytamoxifen in endometrial cancer cells. *Mol Endocrinol* 2006;20:631–46.
- Langer G, Bader B, Meoli L, Isensee J, Delbeck M, Noppinger PR, et al. A critical review of fundamental controversies in the field of GPR30 research. *Steroids* 2010;75:603–10.
- Levin ER. G protein-coupled receptor 30: estrogen receptor or collaborator? *Endocrinology* 2009;150:1563–5.
- Filardo EJ, Graeber CT, Quinn JA, Resnick MB, Giri D, DeLellis RA, et al. Distribution of GPR30, a seven membrane-spanning estrogen receptor, in primary breast cancer and its association with clinicopathologic determinants of tumor progression. *Clin Cancer Res* 2006;12:6359–66.
- Liu Q, Li JG, Zheng XY, Jin F, Dong HT. Expression of CD133, PAX2, ESA, and GPR30 in invasive ductal breast carcinomas. *Chin Med J (Engl)* 2009;122:2763–9.
- Kuo WH, Chang LY, Liu DL, Hwa HL, Lin JJ, Lee PH, et al. The interactions between GPR30 and the major biomarkers in infiltrating ductal carcinoma of the breast in an Asian population. *Taiwan J Obstet Gynecol* 2007;46:135–45.
- Ariazi EA, Brailoiu E, Yerrum S, Shupp HA, Slifker MJ, Cunliffe HE, et al. The G protein-coupled receptor GPR30 inhibits proliferation of estrogen receptor-positive breast cancer cells. *Cancer Res* 2010;70:1184–94.
- Vivacqua A, Lappano R, De Marco P, Sisci D, Aquila S, De Amicis F, et al. G protein-coupled receptor 30 expression is up-regulated by EGF and TGF alpha in estrogen receptor alpha-positive cancer cells. *Mol Endocrinol* 2009;23:1815–26.
- Ahola TM, Purmonen S, Pennanen P, Zhuang YH, Tuohimaa P, Ylikomi T. Progesterone upregulates G-protein-coupled receptor 30 in breast cancer cells. *Eur J Biochem* 2002;269:2485–90.
- Ahola TM, Manninen T, Alkio N, Ylikomi T. G protein-coupled receptor 30 is critical for a progesterone-induced growth inhibition in MCF-7 breast cancer cells. *Endocrinology* 2002;143:3376–84.
- Kimura M, Mizukami Y, Miura T, Fujimoto K, Kobayashi S, Matsuzaki M. Orphan G protein-coupled receptor, GPR41, induces apoptosis via a p53/Bax pathway during ischemic hypoxia and reoxygenation. *J Biol Chem* 2001;276:26453–60.
- Ding Q, Gros R, Limbird LE, Chorazyczewski J, Feldman RD. Estradiol-mediated ERK phosphorylation and apoptosis in vascular smooth muscle cells requires GPR30. *Am J Physiol Cell Physiol* 2009;297:C1178–87.
- Chan QK, Lam HM, Ng CF, Lee AY, Chan ES, Ng HK, et al. Activation of GPR30 inhibits the growth of prostate cancer cells through sustained activation of Erk1/2, c-jun/c-fos-dependent upregulation of p21, and induction of G(2) cell-cycle arrest. *Cell Death Differ* 2010;17:1511–23.
- Recchia AG, De Francesco EM, Vivacqua A, Sisci D, Panno ML, Andò S, et al. The G protein-coupled receptor 30 is up-regulated by hypoxia-inducible factor-1alpha (HIF-1alpha) in breast cancer cells and cardiomyocytes. *J Biol Chem* 2011;286:10773–82.
- Kanda N, Watanabe S. 17Beta-estradiol inhibits oxidative stress-induced apoptosis in keratinocytes by promoting Bcl-2 expression. *J Invest Dermatol* 2003;121:1500–9.
- Swedish Breast Cancer Cooperative Group. Randomized trial of two versus five years of adjuvant tamoxifen for postmenopausal early stage breast cancer. *J Natl Cancer Inst* 1996;88:1543–9.
- Rydén L, Jönsson PE, Chebil G, Dufmats M, Fernö M, Jirstrom K, et al. Two years of adjuvant tamoxifen in premenopausal patients with breast cancer: a randomised, controlled trial with long-term follow-up. *Eur J Cancer* 2005;41:256–64.
- Chebil G, Bendahl PO, Idvall I, Fernö M. Comparison of immunohistochemical and biochemical assay of steroid receptors in primary breast cancer—clinical associations and reasons for discrepancies. *Acta Oncol* 2003;42:719–25.
- Malmström P, Bendahl PO, Boiesen P, Brunner N, Idvall I, Fernö M. S-phase fraction and urokinase plasminogen activator are better markers for distant recurrences than Nottingham Prognostic Index and histologic grade in a prospective study of premenopausal lymph node-negative breast cancer. *J Clin Oncol* 2001;19:2010–9.
- Kotarsky K, Owman C, Olde B. A chimeric reporter gene allowing for clone selection and high-throughput screening of reporter cell lines expressing G-protein-coupled receptors. *Anal Biochem* 2001;288:209–15.
- Sanden C, Broselid S, Cornmark L, Andersson K, Daszkiewicz-Nilsson J, Mårtensson UEA, et al. G protein-coupled estrogen receptor 1/G protein-coupled receptor 30 localizes in the plasma membrane and traffics intracellularly on cytokeleton intermediate filaments. *Mol Pharmacol* 2011;79:400–10.
- Cheng B, Maffi SK, Martinez AA, Acosta YP, Morales LD, Roberts JL. Insulin-like growth factor-I mediates neuroprotection in proteasome inhibition-induced cytotoxicity in SH-SY5Y cells. *Mol Cell Neurosci* 2011;47:181–90.

33. Schoenfeld D. Partial residuals for the proportional hazards regression model. *Biometrika* 1982;69:239–41.
34. Klintman M, Bendahl PO, Grabau D, Lövgren K, Malmström P, Fernö M, et al. The prognostic value of Ki67 is dependent on estrogen receptor status and histological grade in premenopausal patients with node-negative breast cancer. *Mod Pathol* 2010;23:251–9.
35. Cheng SB, Quinn JA, Graeber CT, Filardo EJ. Down-modulation of the G-protein-coupled estrogen receptor, GPER, from the cell surface occurs via a trans-Golgi-proteasome pathway. *J Biol Chem* 2011;286:22441–55.
36. Junttila MR, Evan GI. p53—a Jack of all trades but master of none. *Nat Rev Cancer* 2009;9:821–9.
37. Bologna CG, Revankar CM, Young SM, Edwards BS, Arterburn JB, Kiselyov AS, et al. Virtual and biomolecular screening converge on a selective agonist for GPR30. *Nat Chem Biol* 2006;2:207–12.
38. Holm A, Grände PO, Ludueña RF, Olde B, Prasad V, Leeb-Lundberg LM, et al. The G protein-coupled oestrogen receptor 1 agonist G-1 disrupts endothelial cell microtubule structure in a receptor-independent manner. *Mol Cell Biochem* 2012;366:239–49.
39. Wang C, Lv X, Jiang C, Davis JS. The putative G-protein coupled estrogen receptor agonist G-1 suppresses proliferation of ovarian and breast cancer cells in a GPER-independent manner. *Am J Transl Res* 2012;4:390–402.
40. Carmeci C, Thompson DA, Ring HZ, Francke U, Weigel RJ. Identification of a gene (GPR30) with homology to the G-protein-coupled receptor superfamily associated with estrogen receptor expression in breast cancer. *Genomics* 1997;45:607–17.
41. Agarwal ML, Agarwal A, Taylor WR, Stark GR. p53 controls both the G₂/M and the G₁ cell cycle checkpoints and mediates reversible growth arrest in human fibroblasts. *Proc Natl Acad Sci U S A* 1995;92:8493–7.
42. Tu G, Hu D, Yang G, Yu T. The correlation between GPR30 and clinicopathologic variables in breast carcinomas. *Technol Cancer Res Treat* 2009;8:231–4.
43. Ignatov A, Ignatov T, Weissenborn C, Eggemann H, Bischoff J, Semczuk A, et al. G-protein-coupled estrogen receptor GPR30 and tamoxifen resistance in breast cancer. *Breast Cancer Res Treat* 2011;128:457–66.
44. Miller LD, Liu ET. Expression genomics in breast cancer research: microarrays at the crossroads of biology and medicine. *Breast Cancer Res* 2007;9:206.
45. Krakstad C, Trovik J, Wik E, Engelsen IB, Werner HM, Birkeland E, et al. Loss of GPER identifies new targets for therapy among a subgroup of ER α -positive endometrial cancer patients with poor outcome. *Br J Cancer* 2012;106:1682–8.
46. Ignatov A, Ignatov T, Roessner A, Costa SD, Kalinski T. Role of GPR30 in the mechanisms of tamoxifen resistance in breast cancer MCF-7 cells. *Breast Cancer Res Treat* 2010;123:87–96.
47. Meijer D, van Agthoven T, Bosma PT, Nooter K, Dorssers LC. Functional screen for genes responsible for tamoxifen resistance in human breast cancer cells. *Mol Cancer Res* 2006;4:379–86.
48. van Agthoven T, Sieuwerts AM, Meijer-van Gelder ME, Look MP, Smid M, Veldscholte J, et al. Relevance of breast cancer antiestrogen resistance genes in human breast cancer progression and tamoxifen resistance. *J Clin Oncol* 2009;27:542–9.